EARTHQUAKE ENGINEERING AND STRUCTURAL DYNAMICS
Earthquake Engng. Struct. Dyn. **27**, 845–867 (1998)

MODELLING ASPECTS OF STRUCTURES ISOLATED WITH THE FRICTIONAL PENDULUM SYSTEM

JOSÉ L. ALMAZÁN[1,†], JUAN C. DE LA LLERA[1,*,‡] AND JOSÉ A. INAUDI[2,§]

[1] *Department of Structural Engineering, The Catholic University of Chile, Casilla 306, Correo 22, Santiago, Chile*
[2] *Department of Civil Engineering, University of California at Berkeley, Berkeley, CA, U.S.A.*

SUMMARY

Different modelling aspects of structures isolated using the frictional pendulum system and subjected to earthquake ground motions are studied herein. Although the vertical dynamics of these structures is given special emphasis, other effects such as large isolator deformations and bidirectional input motion are also considered. Different structural models of the FPS are developed and tested for single-storey structures and a real four-storey building frame; among them, an 'exact' formulation of the FPS force–deformation constitutive relationship is presented. Results show that global building responses can be computed within 20 per cent error in the mean using a simplified model that ignores the vertical motion of the building; however, structural member deformations and forces need to be computed using a model that considers such motion. This is of particular importance when there exist correlation between the horizontal and vertical components of ground motion. Further, a physical model of the FPS is introduced and used to determine the response of a real four-storey frame, including uplift and downward impact. Results from this analysis show that local column responses may vary substantially depending on the stiffness of the isolation storey and the presence of a mass at the isolation level. Such mass is capable of filtering the large increase in column shear that results from the impact of the structure after uplift. Uplift occurs at several instants of the response of the structure considered, leading to an increase in column base shear as large as 3 times the shear obtained by ignoring the vertical dynamics of the building. © 1998 John Wiley & Sons, Ltd.

KEY WORDS: frictional pendulum system; base isolation; physical model; uplift; normal forces

INTRODUCTION

Coulomb friction has proven to be a simple and reliable mean of vibration isolation and energy dissipation in earthquake engineering applications. Frictional forces developed at the interphase of two sliding materials are well understood in their functional dependency with contact pressure and sliding velocity.[1,2]

Among the seismic isolation devices based on friction as means of energy dissipation, a remarkable kind is the widely known Frictional Pendulum System (FPS).[3–5] This system consists of a spheric stainless steel surface and a lentil-shaped articulated slider covered by a Teflon-based high bearing capacity composite

* Correspondence to: Juan C. de la Llera, Department of Structural and Geotechnical Engineering, Pontificia Universidad Catolica de Chile, Casilla 306, Correo 22, Santiago, Chile
† Ph.D. Student
‡ Assistant Professor
§ Research Associate

Contract/grant sponsor: FONDECYT; Contract/grant numbers: 1950987, 1971078
Contract/grant sponsor: FONDEF; Contract/grant number: D96I1008

CCC 0098–8847/98/080845–23$17·50

Received 1 August 1997

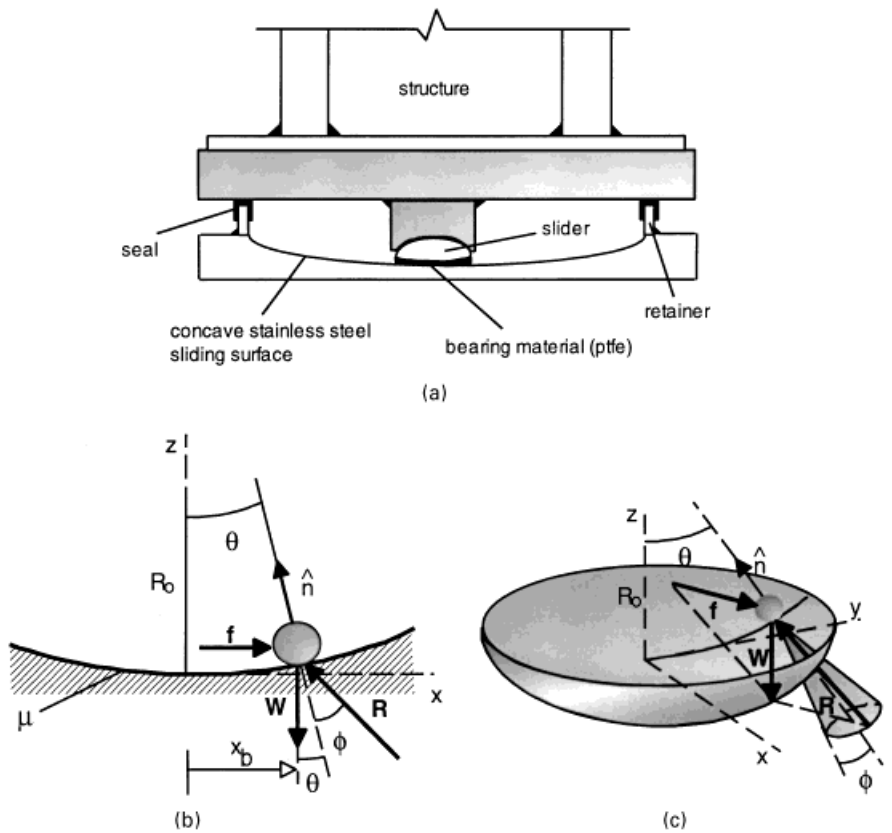

Figure 1. Schematic view of the FPS and equilibrium diagrams in the 2-D and 3-D cases: (a) schematic section of a typical FPS; (b) planar model; (c) three-dimensional model

material (Figure 1(a)). Perhaps, one of the most relevant features of the FPS is that residual displacements in the isolation are reduced due to the self-centering action induced by the concave spherical surface. Residual displacements are an important drawback of other sliders in general. A complete description of the advantages of the FPS system relative to other isolators may be found elsewhere.[2,4]

Several structures have been built in recent years using FPS isolators or devices alike. An interesting, well documented, and recent case is the historic Ninth Circuit U.S. Court of Appeals building located in San Francisco,[2] damaged during the Loma Prieta earthquake in 1989 and retrofitted recently using 256 FPS isolators.

Over the past 10 years the FPS has been studied analytically and experimentally by a number of researchers.[3, 4, 6, 7] Earlier studies developed simplified analytical models capable of representing the predominantly bilinear behaviour of these isolators.[3, 4] They also showed that these models led to results in agreement with measured global responses of shake table tests. Recently, large-scaled tests have been performed at NCEER, Buffalo, on a six- and seven-storey steel frame supported by FPS.[7] Again, results of these tests have been correlated well with global analytical results. Further, some experimental results[3] insinuate that torsional effects would be naturally controlled in structures with FPS, at least for mass eccentric systems.

In spite of the thorough work already done to understand the dynamic behaviour of structures isolated with the FPS system, there are still important aspects of the behaviour of such structures that need further

investigation. Indeed, the vertical vibration of a structure supported by FPS is especially important, since the local behaviour of the isolators is dependent on the contact pressure between the slider and the steel surface. Although such effect have been shown to affect only slightly the global response of a 2D-frame,[7] they do affect the local behaviour and design of the isolators and, hence, deserve special attention from the designer. Moreover, variability in the contact pressure among isolators due to overturning or vertical input motion may induce coupled lateral-torsional vibrations and uplift that need to be better understood. Besides, given the powerful computational tools available today it is possible to formulate an exact solution of the motion of system isolated with the FPS. Such solution can be built in consecutive steps of increasing complexity to better appreciate the approximations implicit in the models available in practice today for predicting the response of FPS isolated structures.

Consequently, the objective of this investigation is to develop a theoretically 'exact' model of the FPS system and relate such model with those developed earlier and used in practice today. Among the modelling issues studied herein, the vertical dynamic behaviour of structures with the FPS system is given special attention. Other modelling aspects, such as biaxial effects, large deformations, and uplift, are also dealt with and analysed. Besides, a physical model of the FPS is presented and briefly discussed; such model provides a simple way to account for uplift and coupled lateral–vertical vibrations of structures isolated with the FPS. Finally, a multistorey building example is analysed and the results compared among different models. This example points out some important issues of the behaviour of these systems that need to be considered by the designer.

Structural responses are studied for a group of six selected earthquake motions. Among them, three recent California earthquake records are considered, which show correlation between lateral and vertical components. This correlation turns out to be an important parameter in assessing the significance of lateral–vertical coupling in the response of the structure. Because such correlation is not as much present in other conventional motions used in earlier investigations of the FPS, it is interesting to see the implications of such effect in the global as well as local response of the structural system. Furthermore, the large displacements observed in these near-field earthquake records may induce large displacement effects on the FPS that need to be considered appropriately in the modelling.

FORCE–DEFORMATION CONSTITUTIVE RELATION OF THE FPS

An important aspect in formulating the complete equations of motion of systems isolated with the FPS, is to state the exact force–deformation constitutive relationship of the isolator. Indeed, the different levels of complexity involved in formulating this relationship are directly related with the accuracy of the model. In the formulation presented displacements are imposed to the FPS and forces are retrieved from it.

Let us state first the well-known force–deformation relationship of the FPS system in one dimension and small deformation (Figure 1(b)), which results from horizontal equilibrium of the isolator.[3, 4]

$$f = \frac{W}{R_o} x_b + \mu W \operatorname{sgn}(\dot{x}_b) \tag{1}$$

where W represents the weight of the structure acting on the isolator; x_b and $\dot{x}_b$ are the lateral deformation and velocity of the isolator relative to the ground, respectively; R_o is the radius of the spherical surface; μ is the friction coefficient; $\operatorname{sgn}(\dot{x}_b)$ is the signum function, i.e., equal to -1 or $+1$ depending if the velocity is negative or positive, respectively; and f is the horizontal restoring force of the isolator. Equation (1) is derived assuming that the angle θ between the normal and the vertical direction is small (Figure 1(b))—thus, $\cos(\theta) = 1$ and $\mu \tan(\theta) \approx 0$. Based on this assumption the normal contact force N, is implicitly assumed equal to W. Naturally, such approximation is valid only when the vertical component of ground motion is ignored.

Equation (1) may be extended to the case of bidirectional motion of the isolator by stating the conditions of dynamic equilibrium in the horizontal plane, leading to:

$$\mathbf{f} = \frac{W}{R_o}\,\mathbf{q}_h + \mu W\,\frac{\dot{\mathbf{q}}_h}{\|\,\dot{\mathbf{q}}_h\,\|} \tag{2}$$

again, $\mathbf{f} = [f_x\ f_y]^T$ is the horizontal restoring force of the isolator, where f_x and f_y are the cartesian components of this force in the x and y directions, respectively; $\mathbf{q}_h = [x_b\ \ y_b]^T$ is the horizontal deformation of the isolator relative to the ground with x- and y-components x_b and y_b; and $\dot{\mathbf{q}}_h = [\dot{x}_b\ \ \dot{y}_b]^T$ is the horizontal velocity of the FPS. The similarity between equations (1) and (2) is obvious when identifying $\mathrm{sgn}(\dot{x}_b)$ with $\dot{\mathbf{q}}_h/\|\,\dot{\mathbf{q}}_h\,\|$, the latter corresponding to a unitary vector tangent to the horizontal isolator trajectory. Both equations (1) and (2) are limited to small isolator deformations.

By using the actual displaced geometry, equation (2) may be extended to the most general case of large isolator deformations. Horizontal dynamic equilibrium of the isolator in that case leads to (Figure 1(c)):

$$\mathbf{f} = \frac{N}{\rho}\,\mathbf{q}_h + \mu N\,\frac{\dot{\mathbf{q}}_h}{\|\,\dot{\mathbf{q}}\,\|} \tag{3}$$

where N is the magnitude of the normal contact force, ρ is the radius of curvature of the concave surface—this radius is constant and equal to R_o for the FPS system; however, the formulation presented is not limited to such case; and $\dot{\mathbf{q}} = [\dot{x}_b\ \ \dot{y}_b\ \ \dot{z}_b]^T$ is the true velocity of the isolator relative to the ground, where $\dot{z}_b$ is its vertical component. This latter velocity term results from imposing the kinematic constraint corresponding to the motion of the isolator on the spherical (or arbitrary) sliding surface; its value depends on the horizontal displacement $\mathbf{q}_h$ and velocity $\dot{\mathbf{q}}_h$ of the FPS.

It is important to note in equation (3) that the reaction N is no longer constant and equal to the weight W. The value of this reaction is continuously varying during the motion of the system due to the vertical component of ground motion and the lateral–vertical coupling that exists between the horizontal and vertical motion of the FPS. Moreover, since the isolator deformation $\mathbf{q}_h$ and velocity $\dot{\mathbf{q}}_h$ are imposed by the structure, the only unknown at the element level is the magnitude of the normal reaction N.

In general, equations (1)–(3) show that the horizontal restoring force of the isolator comes from the superposition of two different actions, one resulting from the pendular effect associated to the centering action of the weight W, $\mathbf{f}_p$, and the other, resulting from the frictional forces developed at the isolator interface between the slider and surface, $\mathbf{f}_\mu$. Thus, equation (1)–(3) may be expressed more synthetically as

$$\mathbf{f} = \mathbf{f}_p + \mathbf{f}_\mu \tag{4}$$

Equations (1)–(4) represent the horizontal restoring force of the isolator when it is sliding on the concave surface. During the sliding phase of motion, the frictional force $\mathbf{f}_\mu$ always opposes to the direction of the velocity implying that the total reaction $\mathbf{R}$ at the sliding surface, whose component of the tangent plane is the frictional force, is always located on the surface of the friction cone (Figures 1(b) and 1(c)). This reaction changes direction continuously following the isolator trajectory; however, since the angle ϕ between the normal to the surface $\hat{n}$ and the reaction $\mathbf{R}$ at a given point is fixed —$\phi = \tan^{-1}(\mu)$—, as soon as the angle between the resultant external force and the normal $\hat{n}$ is larger than ϕ, the magnitude of the isolator velocity will increase. On the other hand, if the angle between the resultant of the external forces and the normal $\hat{n}$ is smaller than ϕ, the isolator velocity will decrease until it stops and sticks to the concave surface. From there on, the structure will function as a fixed-base system. In the sticking range, the reaction $\mathbf{R}$ will be that required to maintain equilibrium with the external resultant. During the actual motion of the system, the isolator will shift between these two phases, i.e., a sticking phase (phase I) and a sliding phase (phase II).

STRUCTURAL SYSTEMS AND RESPONSES CONSIDERED

The structural model considered first corresponds to a single-storey building isolated with one FPS (Figure 2(a)). The masses of the structure and the base are m_s and m_b, respectively, and their ratio will be be defined as $\alpha = m_b/m_s$. As shown in the figure, the columns between the floor and isolation levels are modelled by springs and dashpot elements in three perpendicular directions, the two horizontal x and y, and the vertical z.

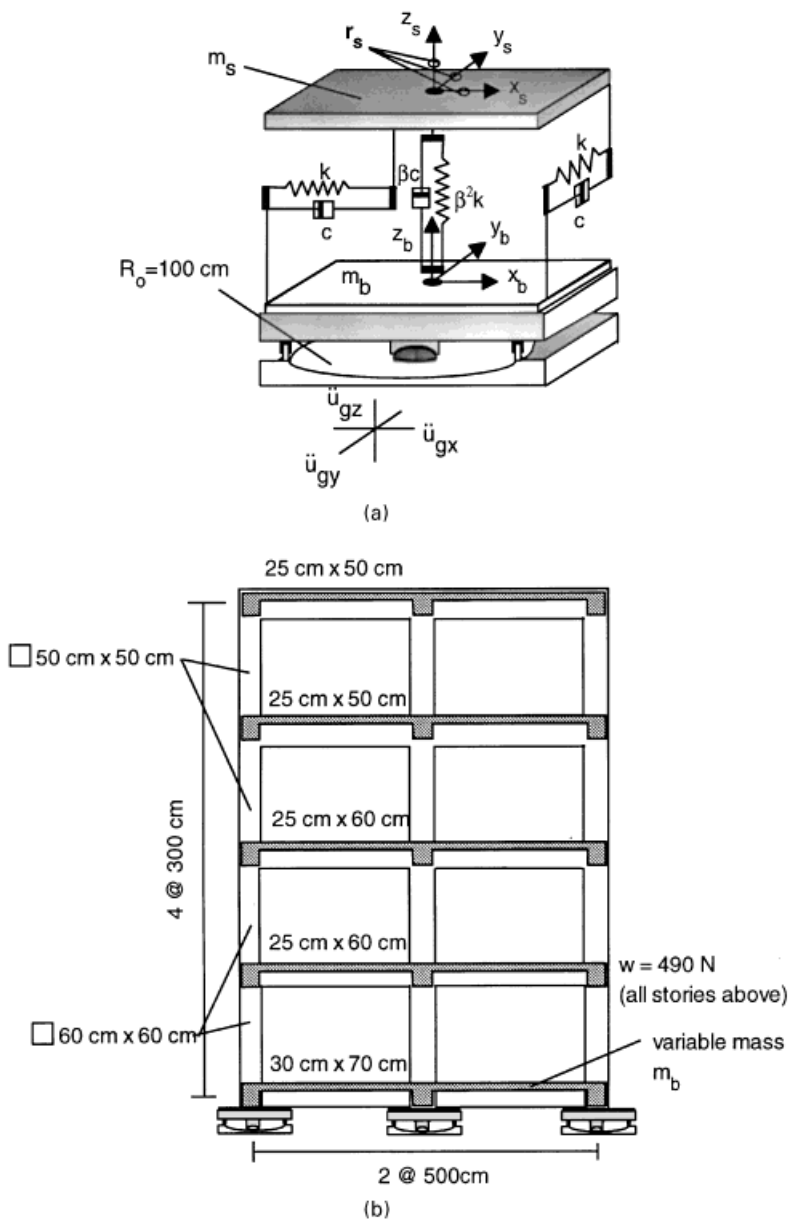

Figure 2. Schematic view of the systems considered: (a) single-storey system considered in parametric study; and (b) four-storey building frame used in example

Table I. Structural models considered in this study

Case model	Constitutive relationship	Structural model		Observations
		Simplified	Exact	
I	Equation (2)	√		$N = W$
II	Equation (2)	√		$N = W\,(1 + \ddot{u}_{gz}/g)$
III	Equation (3)	√		Exact N
IV	Equation (3)		√	Exact N

Two main structural models are considered in this study. First, a 'simplified' structural model which neglects the vertical response of the system by imposing infinite axial stiffness in the building columns. And second, an 'exact' model which considers the lateral and vertical motion of the system using the actual horizontal as well as vertical stiffness of columns. In turn, both structural models are combined with different models of the force–deformation constitutive relationship of the FPS system, leading to the four analysis cases described in Table I.

Thus, case I represents a building with infinite axial stiffness in columns and connected to an FPS isolator modelled assuming small deformations and a constant normal contact force equal to the weight above the isolator, $W = (m_s + m_b)\,g$. Case II is similar to I but includes the vertical component of ground acceleration in the computation of the normal contact force. This model has been considered in earlier investigations.[7] Furthermore, case III is identical to cases I and II but considers the exact value of the normal contact force N assuming large deformations in the isolator but infinite vertical stiffness of columns. Finally, case IV considers the exact solution including large deformations of the isolator and finite vertical stiffness of the structure.

The deformations of the structure relative to the ground will be denoted as $\mathbf{r} = [x_s\ y_s\ z_s]^T = [\mathbf{r}_h\ z_s]^T$, and the deformations of the base relative to the ground as $\mathbf{q} = [x_b\ y_b\ z_b]^T = [\mathbf{q}_h\ z_b]^T$, where $\mathbf{r}_h$ and $\mathbf{q}_h$ represent a partition containing the two horizontal degrees of freedom of the structure and base, respectively. The corresponding mass, damping, and stiffness matrices of the fixed-base structure will be denoted as $\mathbf{M}_s$, $\mathbf{C}_s$ and $\mathbf{K}_s$; a consistent partition of these matrices with $\mathbf{r}_h$ and z_s is as follows:

$$\mathbf{M}_s = \begin{bmatrix} \mathbf{M}_{sh} & 0 \\ 0 & m_z \end{bmatrix}, \quad \mathbf{C}_s = \begin{bmatrix} \mathbf{C}_{sh} & 0 \\ 0 & c_z \end{bmatrix}, \quad \mathbf{K}_s = \begin{bmatrix} \mathbf{K}_{sh} & 0 \\ 0 & k_z \end{bmatrix} \tag{5}$$

where $\mathbf{M}_{sh}$, $\mathbf{C}_{sh}$, and $\mathbf{K}_{sh}$ are the mass, damping, and stiffness matrices associated with the horizontal degrees of freedom of the superstructure; $m_z = m_s$, the translational mass of the structure, $c_z = \beta c_s$, the damping coefficient of the structure; and $k_z = \beta^2\,k_s$, the lateral stiffness of the structure, where $\beta = \omega_v/\omega_o$ represents the ratio between the vertical and horizontal vibration frequency of the structure—typical values for β in frame buildings range between 5 and 15.

System responses were computed for six different free field ground motion records. The motions considered were Viña de Mar and Llolleo (Chile, 1985), Corralitos (Loma Prieta, 1989), Sylmar and Newhall (Northridge, 1994), and Kobe University (Kobe, 1995). The three ground acceleration components of these motions are presented in Figure 3. Since the selected recorded motions of the Kobe earthquake correspond to ground velocity, ground acceleration have been computed by numerical differentiation of this original record. The reader is warned that in the case of the vertical component of the Llolleo record (Chile, 1985), the initial part of the vertical component has been omitted due to the apparent faulty sensor functioning; in spite of that, the remaining unperturbed section of the record has been included because of its great interest for structures subjected to earthquakes originated in subduction zones and founded on stiff soils.

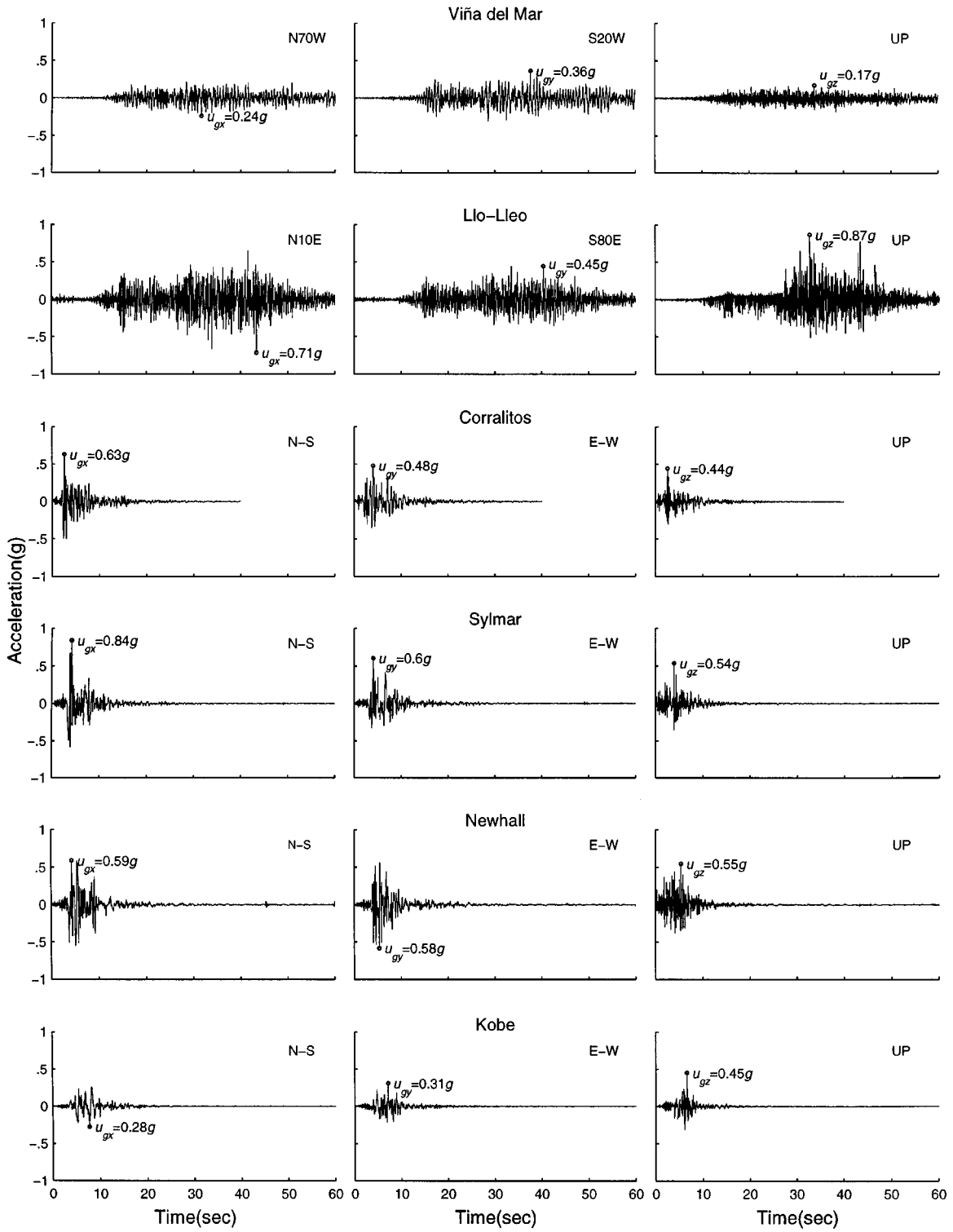

Figure 3. Ground motion records considered in this study

The results presented in this study consider a constant value of the friction coefficient[2,7] $\mu = 0{\cdot}07$. Although including the variability of μ with velocity and pressure as proposed in earlier work[1] does not imply any extra difficulty in the model, it seemed unnecessary due to the minor effect that the variation in μ has on the peak response values of the system. Further, a constant damping ratio $\xi = 0{\cdot}05$ was considered for the superstructure in all analysis cases.

The system responses considered in this study are: (1) the normalized horizontal deformation $\hat{\mathbf{q}}_h = \mathbf{q}_h/\mathbf{R}_o$ of the isolation level relative to the ground, (2) the normalized horizontal restoring force $\hat{\mathbf{f}} = \mathbf{f}/\mathbf{W}$ of the isolator, (3) the normalized base shear $\hat{\mathbf{V}} = \mathbf{V}/(\mathbf{m}_s\,\mathbf{g})$ of the structure, and (4) the normalized contact reaction in the isolator $\hat{\mathbf{N}} = \mathbf{N}/\mathbf{W}$ normal to the sliding surface. Because of the mass m_b lumped at the isolation level, it is important to emphasize that the horizontal restoring force on the isolator $\mathbf{f}$ is different from the total base shear $\mathbf{V}$ of the structure; the difference being the inertia force generated at the base.

EQUATIONS OF MOTION

Next, the general equations of motion of the two structural models described above are stated and interpreted. For each structural model, the sticking (phase I) and sliding (phase II) phases of the motion are identified and the corresponding equations presented. In the most general case, the degrees of freedom of the system are five; three degrees of freedom of the superstructure and two degrees of freedom of the isolated base. The degrees of freedom of the structure and base will be denoted as $\mathbf{d} = [\mathbf{r}_h\ z_s\ \mathbf{q}_h]^T = [\mathbf{r}\ \mathbf{q}_h]^T$, and the corresponding velocities and accelerations as $\dot{\mathbf{d}}$ and $\ddot{\mathbf{d}}$.

During the sticking phase, the governing equations of motions of the system correspond to that of a fixed-base structure. For a structure with infinite vertical stiffness in columns, the equations are:

$$\mathbf{M}_{sh}\,\ddot{\mathbf{r}}_h + \mathbf{C}_{sh}\,\dot{\mathbf{r}}_h + \mathbf{K}_{sh}\,\mathbf{r}_h = -\mathbf{M}_{sh}\,\ddot{\mathbf{u}}_{gh} - \mathbf{K}_{sb}\,(1{:}2,\ 1{:}2)\,\mathbf{q}_h \tag{6}$$

and for a structure with finite vertical stiffness in columns,

$$\mathbf{M}_s\,\ddot{\mathbf{r}} + \mathbf{C}_s\,\dot{\mathbf{r}} + \mathbf{K}_s\,\mathbf{r} = -\mathbf{M}_s\,\ddot{\mathbf{u}}_g - \mathbf{K}_{sb}\,\mathbf{q} \tag{7}$$

where $\mathbf{K}_{sb}$ represents the off-diagonal matrix coupling $\mathbf{r}$ and $\mathbf{q}$; and the notation $(i{:}j,\ k{:}l)$ represents the submatrix delimited between rows i and j and columns k and l. These equations are essentially identical to those of a fixed-base structure but include the shift in position of the slider $\mathbf{q}$ at the time of the last sticking.

Pre-multiplying equations (6) and (7) by the inverse of the mass matrix $\mathbf{M}_s$, equation (6) can be written in parametric form as

$$\ddot{\mathbf{r}}_h + 2\xi\omega_o\,\dot{\mathbf{r}}_h + \omega_o^2\,\mathbf{r}_h = -\ddot{\mathbf{u}}_{gh} - \omega_o^2\,\mathbf{q}_h \tag{8}$$

and equation (7) as

$$\begin{bmatrix}\ddot{\mathbf{r}}_h\\ \ddot{z}_s\end{bmatrix} + 2\xi\omega_o\begin{bmatrix}\mathbf{I}_{2\times 2} & \mathbf{0}\\ \mathbf{0} & \beta\end{bmatrix}\begin{bmatrix}\dot{\mathbf{r}}_h\\ \dot{z}_s\end{bmatrix} + \omega_o^2\begin{bmatrix}\mathbf{I}_{2\times 2} & \mathbf{0}\\ \mathbf{0} & \beta^2\end{bmatrix}\begin{bmatrix}\mathbf{r}_h\\ z_s\end{bmatrix}$$

$$= -\begin{bmatrix}\ddot{\mathbf{u}}_{gh}\\ \ddot{u}_{gz}\end{bmatrix} - \omega_o^2\begin{bmatrix}\mathbf{I}_{2\times 2} & \mathbf{0}\\ \mathbf{0} & \beta^2\end{bmatrix}\begin{bmatrix}\mathbf{q}_h\\ z_b\end{bmatrix} \tag{9}$$

In equation (9), the vertical displacement of the isolation base z_b is such that it satisfies the kinematic constraint imposed by the sliding surface, i.e., $G(x_b,\ y_b,\ z_b) = 0$. For convenience, z_b is chosen as the dependent variable of $\mathbf{q}_h$, implying that $z_b = g(\mathbf{q}_h)$.

On the other hand, the FPS horizontal restoring force $\mathbf{f}$ can be directly computed from equilibrium at the isolation base for both structure models as

$$\mathbf{f} = -[K_{sb}^{T}(1:2, 1:2)\,\mathbf{r}_h + \mathbf{K}_b(1:2, 1:2)\,\mathbf{q}_h + \mathbf{C}_{sb}^{T}(1:2, 1:2)\,\dot{\mathbf{r}}_h + \mathbf{M}_{bh}\,\ddot{\mathbf{u}}_{gh}] \tag{10}$$

where $\mathbf{K}_b$ represents the submatrix of stiffness associated with the deformations $\mathbf{q}$ of the isolated base; $\mathbf{C}_{sb}$ is the damping submatrix coupling the $\dot{\mathbf{r}}$ and $\dot{\mathbf{q}}$ velocities; and $\mathbf{M}_{bh}$ is the mass submatrix associated with $\ddot{\mathbf{q}}_h$.

Equations (5)–(9) can be used as long as the horizontal restoring force $\mathbf{f}$ of the FPS does not exceed the frictional resistance developed by the isolator. The condition of sticking can be simply stated saying that the reaction at a given point on the surface must remain within the friction cone (Figure 1(c)). This leads to the following condition for sticking:

$$\| \mathbf{R} - N\,\hat{\mathbf{n}} \| < \mu N \tag{11}$$

where $\mathbf{R}$ is the total reaction developed at the sliding surface of the isolator; $N = \mathbf{R} \cdot \hat{\mathbf{n}}$ is the magnitude of the reaction normal to the tangent plane at the point considered; and $\| (\cdot) \|$ represents the euclidean norm of the vector. For instance, the value of the vertical component of the reaction, R_z, is obtained from equilibrium with the vertical action imposed by the structure onto the FPS $f_z = k_z (z_s - z_b) + c_z \dot{z}_s$, the vertical inertia force acting on the base $m_b \ddot{u}_{gz}$, and the weight of the structure $(m_s + m_b)\,g$. In the case of small deformations, equation (11) is simplified to

$$\left\| \mathbf{f} - \frac{W}{R_o}\,\mathbf{q}_h \right\| < \mu W \tag{12}$$

Next, the complete equations of the sliding motion of the structural system shown in Figure 2(a) are stated. The degrees of freedom considered are 4, both horizontal deformations of the structure and base, or 5, i.e., $\mathbf{d} = [\mathbf{r}\ \mathbf{q}_h]^T$, if the vertical deformation of the structure is included. Recall that the vertical deformation, velocity, and acceleration of the base relative to the ground z_b, $\dot{z}_b$, and $\ddot{z}_b$, are kinematically dependent of the horizontal deformations $\mathbf{q}_h$ of the FPS.

In order to reduce the number of equations presented, a general formulation of a structure sliding on the FPS is presented; the formulation for the 'simplified' structural system having infinite axial stiffness in the columns can be obtained directly from the more general equation presented by eliminating the row and column corresponding to the vertical degree of freedom z_s of the structure:

$$\begin{bmatrix} \mathbf{M}_s & \mathbf{0} \\ \mathbf{0} & \mathbf{M}_{bh} \end{bmatrix} \begin{bmatrix} \ddot{\mathbf{r}} \\ \ddot{\mathbf{q}}_h \end{bmatrix} + \begin{bmatrix} \mathbf{C}_s & \mathbf{C}_{sb}(:, 1:2) \\ \mathbf{C}_{sb}^{T}(:, 1:2) & \mathbf{C}_b(1:2, 1:2) \end{bmatrix} \begin{bmatrix} \dot{\mathbf{r}} \\ \dot{\mathbf{q}}_h \end{bmatrix} + \begin{bmatrix} \mathbf{K}_s & \mathbf{K}_{sb}(:, 1:2) \\ \mathbf{K}_{sb}^{T}(1:2, 1:2) & \mathbf{K}_b(1:2, 1:2) \end{bmatrix} \begin{bmatrix} \mathbf{r} \\ \mathbf{q}_h \end{bmatrix}$$

$$= -\begin{bmatrix} \mathbf{M}_s & \mathbf{0} \\ \mathbf{0} & \mathbf{M}_{bh} \end{bmatrix} \mathbf{B}_u\,\ddot{\mathbf{u}}_g - \begin{bmatrix} \mathbf{K}_{sb}(:, 3) & \mathbf{C}_{sb}(:, 3) \\ \mathbf{0} & \mathbf{0} \end{bmatrix} \begin{bmatrix} z_b \\ \dot{z}_b \end{bmatrix} - \begin{bmatrix} \mathbf{0} \\ \mathbf{f} \end{bmatrix} \tag{13}$$

where $\mathbf{B}_u$ represents the influence matrix of the input, $\mathbf{C}_b$ is the damping matrix associated with the base velocity $\dot{\mathbf{q}}$; and $\mathbf{f}$ is the horizontal restoring force of the isolator computed using equations (2) or (3) depending on the constitutive model considered. The right-hand-side term including z_b and $\dot{z}_b$ in this equation represents the forces applied to the $\mathbf{r}$ degrees of freedom of the structure due to the constrained vertical displacement and velocity of the FPS. As mentioned before, z_b is computed directly from the kinematic constraint $z_b = g(\mathbf{q}_h)$; $\dot{z}_b$ can also be computed directly from this equation:

$$\dot{z}_b = \dot{g}(\mathbf{q}_h, \dot{\mathbf{q}}_h) = \left(\frac{\partial g}{\partial \mathbf{q}_h} \right)^{T} \dot{\mathbf{q}}_h = \frac{\partial g}{\partial x_b}\,\dot{x}_b + \frac{\partial g}{\partial y_b}\,\dot{y}_b \tag{14}$$

Therefore, the r.h.s. term in equation (13) depending on z_b and $\dot{z}_b$, is actually dependent on the horizontal displacements and velocities of the FPS. It is through this term and the horizontal restoring force $\mathbf{f}$ that lateral–vertical coupling is developed in the structural system. The parametric representation of equation (13) is omitted here for the sake of brevity.[8]

COMPUTATION OF THE NORMAL REACTION N

The integration of the equation of motion (13) differs from that of a fixed-base structure due to the computation of the non-linear restoring force $\mathbf{f}$ of the FPS isolator (Equations (1)–(3)). This force depends, in turn, on the normal reaction $\mathbf{N}$ developed at the spherical sliding surface, which magnitude is computed from dynamic equilibrium of the FPS in the direction of the normal $\hat{\mathbf{n}}$ to the concave surface:

$$N = W\ n_z - \Lambda \cdot \hat{\mathbf{n}} + m_b\, \ddot{\mathbf{u}}_g \cdot \hat{\mathbf{n}} + m_b\, a_n \tag{15}$$

where n_z is the vertical component of the normal $\hat{\mathbf{n}}$ to the surface, $a_n = \ddot{\mathbf{q}} \cdot \hat{\mathbf{n}}$ is the normal acceleration of the isolator relative to the ground;[8] and $\Lambda = -m_s\,(\ddot{\mathbf{u}}_g + \ddot{\mathbf{r}})$ is the dynamic interaction force between the superstructure and base. Substituting Λ in equation (15) and defining the relative acceleration of the structure with respect to the isolation $\ddot{\mathbf{r}}_{sb} = \ddot{\mathbf{r}} - \ddot{\mathbf{q}}$, this equation leads to:

$$N = W\ n_z + (m_s + m_b)\ \ddot{\mathbf{u}}_g \cdot \hat{\mathbf{n}} + (m_s + m_b)\, a_n + m_s\ \ddot{\mathbf{r}}_{sb} \cdot \hat{\mathbf{n}} \tag{16}$$

Each term in equation (16) can be physically interpreted. For instance, the first three terms correspond to the normal force produced as if the system were a rigid body. The first term is the component of the weight along the normal direction; the second term is the component of the inertia force generated on the structure as a rigid body by the ground motion; and the third reflects the effect due to the spherical motion of the FPS along the spherical isolator surface. The last term on the r.h.s. of this equation reflects the effect that the flexibility of the structure has on the value of the normal reaction.

So far, the formulation presented assumes that no uplift is produced in the system during the motion, i.e., $N > 0$. Uplift will be introduced in a natural form later through a proposed physical model of the FPS.

INTEGRATION OF THE EQUATIONS OF MOTION

During phase I of the motion of the structure, equations (8) and (9) represent the well-known linear motion of a fixed-base structure. For numerical simplicity these equations are integrated by first transforming them into first-order differential equations (state-space formulation) and using a first-order hold in the integration. Phase changes between sticking and slip are evaluated using equations (11) and (12); thus, for instance, sticking of the structure is produced when zero velocity is reached at the FPS and the frictional force required for equilibrium is less than the maximum frictional force. Next, the integration algorithm is briefly described for the 'exact' model of the structural system considered; other structural model cases are analysed using the same integration procedure.

Let us start assuming that the state of the system, i.e., the displacements $\mathbf{d}(t_k) = [\mathbf{r}(t_k)\ \mathbf{q}_h(t_k)]$ and velocities $\dot{\mathbf{d}}(t_k) = [\dot{\mathbf{r}}(t_k)\ \dot{\mathbf{q}}_h(t_k)]$, are known at instant $t_k = kT$, where T is the integration step. The integration of equation (13) continues as follows: (1) determine the unitary normal vector $\hat{\mathbf{n}}$ to the surface at $x(t_k)$; (2) compute the normal acceleration a_n;[8] (3) determine the interaction force $\Lambda = \mathbf{K}_{sb}^T\,\mathbf{r} + \mathbf{K}_b\,\mathbf{q} + \mathbf{C}_{sb}^T\,\dot{\mathbf{r}} + \mathbf{C}_b\,\dot{\mathbf{q}}$; (4) evaluate the magnitude of the normal reaction N using equation (15); (5) determine the horizontal restoring force $\mathbf{f}$ developed by the FPS using equations (1), (2), or (3); (6) compute the vertical displacement and velocity of the isolator, z_b and $\dot{z}_b$, by equation (14); (7) compute $\ddot{\mathbf{r}}$ and $\ddot{\mathbf{q}}_h$ using equation (13); and (8) compute the state in the next step, $\mathbf{d}(t_{k+1})$ and $\dot{\mathbf{d}}(t_{k+1})$. The last step in the integration procedure depends on the time

integration method used. In this investigation a fourth-order Runge–Kutta method has been selected. In order to use the method, equation (13) was transformed into a first-order differential equation.

ANALYSIS OF RESULTS

The objective of this section is to study parametrically the earthquake behaviour of the single-storey system considered using different structural models. The results presented are intended to evaluate the effect of specific phenomena present in the behaviour of structures isolated using the FPS, such as the effect of large deformations, vertical input, vertical flexibility of the structure, and bidirectional input motion. Although due to the non-linear nature of the coupled equations of motion of the system, it is impossible to isolate and evaluate independently the effect of different modeling assumptions, an effort has been made in presenting results that show how different effects control the earthquake response of these systems.

Let us start considering the unidirectional lateral impulse response of the system with rigid and deformable superstructure. Shown in Figure 4 is a comparison between the normalized horizontal base deformation $\hat{x}_b$, the normalized base velocity $\dot{x}_b(t)/\dot{x}_b(t=0)$, the normalized normal force $\hat{N}$, and the normalized force deformation relationship of the isolator. The parameters of the rigid superstructure model

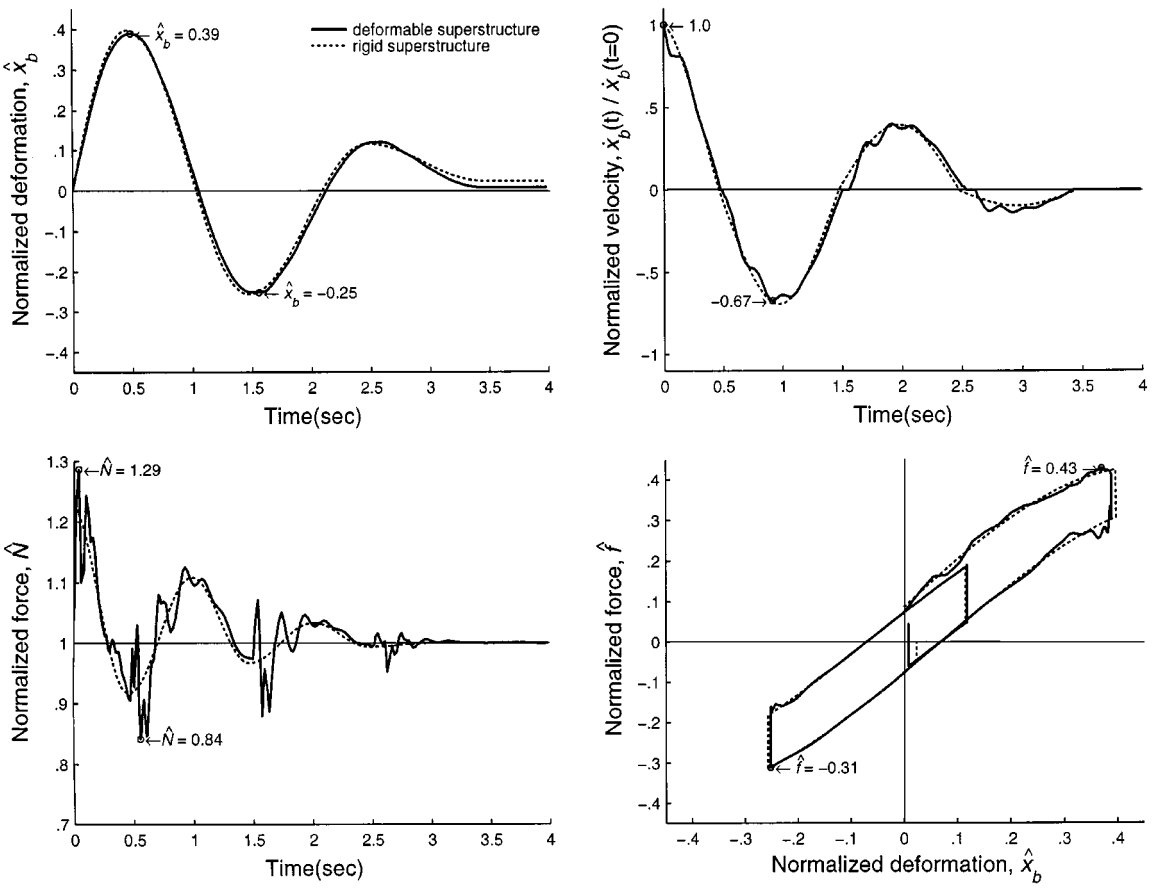

Figure 4. Comparison between the impulse response of the system including ($T_o = 0{\cdot}5$ sec, $\beta = 7$, $\alpha = 0{\cdot}2$) and neglecting ($T_o = 0$ sec, $\beta = \infty$, $\alpha = 0{\cdot}2$) the flexibility of the superstructure

are $T_o = 0$ sec., i.e., $\beta = \infty$, and mass ratio $\alpha = 0.2$; the corresponding parameters of the flexible superstructure are $T_o = 0{\cdot}5$ sec., $\beta = 7$, and $\alpha = 0{\cdot}2$. These results show that differences between the isolator deformations computed from both models are very small; however, slightly larger discrepancies, say 10 per cent, are observed in the normal force as a result of the lateral and vertical flexibility of the system. The change in normal force relative to 1 in the latter model is due to the large displacement effects of the slider moving along the concave surface, the normal acceleration thus produced, and the flexibility of the system (equation (16)). It is also responsible for the interesting waviness shown in the normalized force–deformation relationship of the flexible system.

Because the normal contact force $\hat{N}$ is intuitively expected to affect the earthquake response of the structure, the dynamic variation of this force is evaluated in greater detail. Compared in Figure 5 are the earthquake responses of the structure ($T_o = 0{\cdot}5$ sec, $\alpha = 0{\cdot}2$, $\beta = 7$) obtained from model cases I and IV. Both models are subjected to the Newhall ground motion record; however, in case model I only the two horizontal components are included as opposed to the three components in case model IV. The upper two plots show the interaction between the two components of the frictional force $\mathbf{f}_\mu$ in the isolator; the plots on the left of the figure correspond to results obtained from the approximate model (case I) and those on the right to results

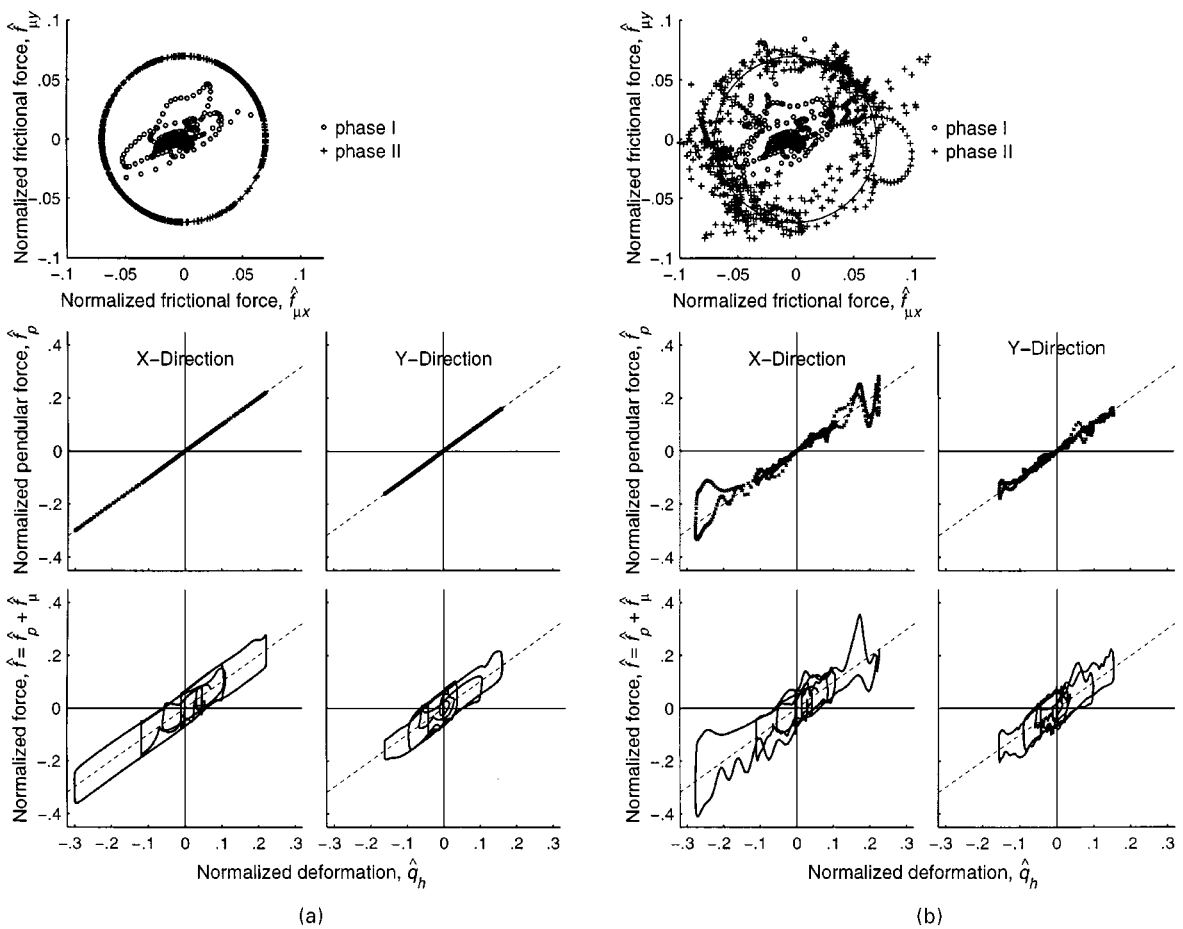

Figure 5. Earthquake response of case models I and IV subjected to the Newhall ground motion ($T_o = 0{\cdot}5$ sec, $\beta = 7$, $\alpha = 0{\cdot}2$) for: (a) case model I; and (b) case model IV

obtained from the exact model (case IV). As it should be, the frictional forces in the simplified model describe a circular interaction; however, since the normal force is continuously varying during the motion of the structure in case model IV, sliding occurs inside as well as outside the circular interaction curve. Indeed, the discrepancies observed between these two plots is a measure of the effect of the variable normal force $\hat{N}$. Notice also that the friction forces during sticking (circles) maintain certain similarity in both case models as opposed to the large discrepancies observed in these forces during sliding (phase II). The second row of plots describes the normalized pendular component $\hat{\mathbf{f}}_p$ of the FPS horizontal restoring force versus the normalized isolator deformation $\hat{\mathbf{q}}_h$. The relationship is linear for the approximate model with $\hat{N} = 1$, and differs from it in the exact model due to the continuous variation in the normal contact force. The last row of plots shows the normalized constitutive force–deformation relating the x- and y-direction isolator force and deformation. The waviness present on the two plots on the right results from the variation in the contact normal force caused by the true modelling of the vertical dynamics of the structure. As shown later, the occurrence of these spikes at large values of displacement can be explained by the correlation between peaks of the horizontal and vertical ground motion components.

Mean spectra of maximum and minimum normalized $\hat{N}$ are presented in Figure 6 for the six ground motions selected. These spectra were computed using the exact structural model (cases IV) and the three components of each ground motion. They are plotted as a function of the fixed-base period of the structure for values of vertical to lateral stiffness ratio $\beta = 5$ and 7, and three values of the mass ratio $\alpha = 0{\cdot}1$, $0{\cdot}2$, and $0{\cdot}5$. As shown in the figure, the mean maximum values of $\hat{N}$ range approximately between $1{\cdot}6$ and 2, implying that amplifications of 50–100 per cent should be expected in the normal contact force during an earthquake. On the other hand, minimum mean values of $\hat{N}$ vary from about $0{\cdot}2$ to $0{\cdot}6$, implying that decreases of the normal contact force of the order of $1/2$ to $1/5$ should also be expected. The peak values of $\hat{N}$ tend to be larger for the maximum and smaller for the minimum in the mid-period range, respectively. Further, these extreme values are quite stable for different values of the vertical-to-lateral stiffness ratio β and mass ratio α.

Now that the variations produced in the value of the normal contact force $\hat{N}$ have been evaluated, it is important to study the effect that these variations may have in the earthquake response of the system. Let us first consider the case of a single structure subjected to the Newhall ground motion (Figure 7). The comparisons presented here are again between the structural case models I and IV (Table I). The structural system considered has a fixed-base period $T_o = 0{\cdot}5$ sec, vertical to lateral stiffness ratio $\beta = 7$, and mass ratio $\alpha = 0{\cdot}2$. The results presented in the figure are the normalized x-direction isolation displacement $\hat{x}_b$ and base shear $\hat{V}_x$, the magnitude of the normalized normal force $\hat{N}$, and the normalized x-direction force–deformation loop. Notice that the horizontal deformations at the isolation level are similar for both structural models

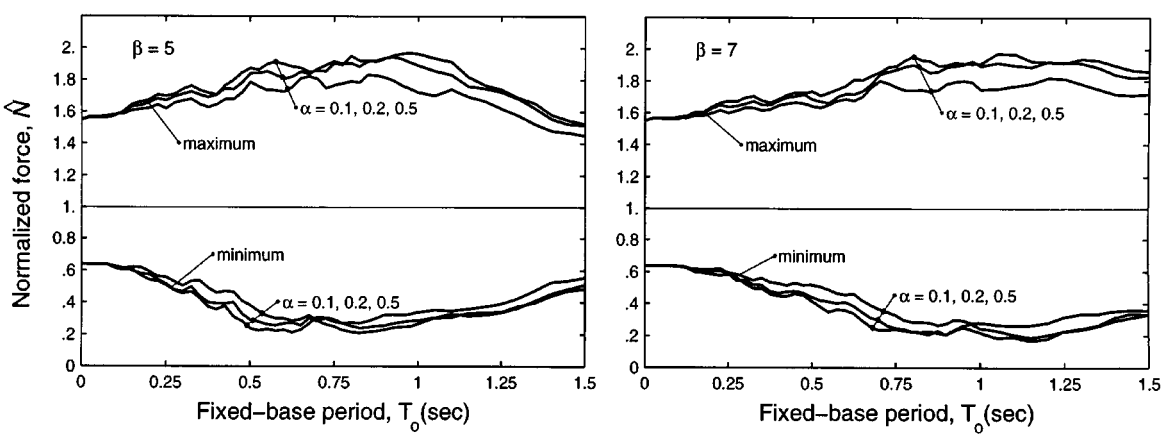

Figure 6. Mean spectra of maximum and minimum normalized force $\hat{N}$

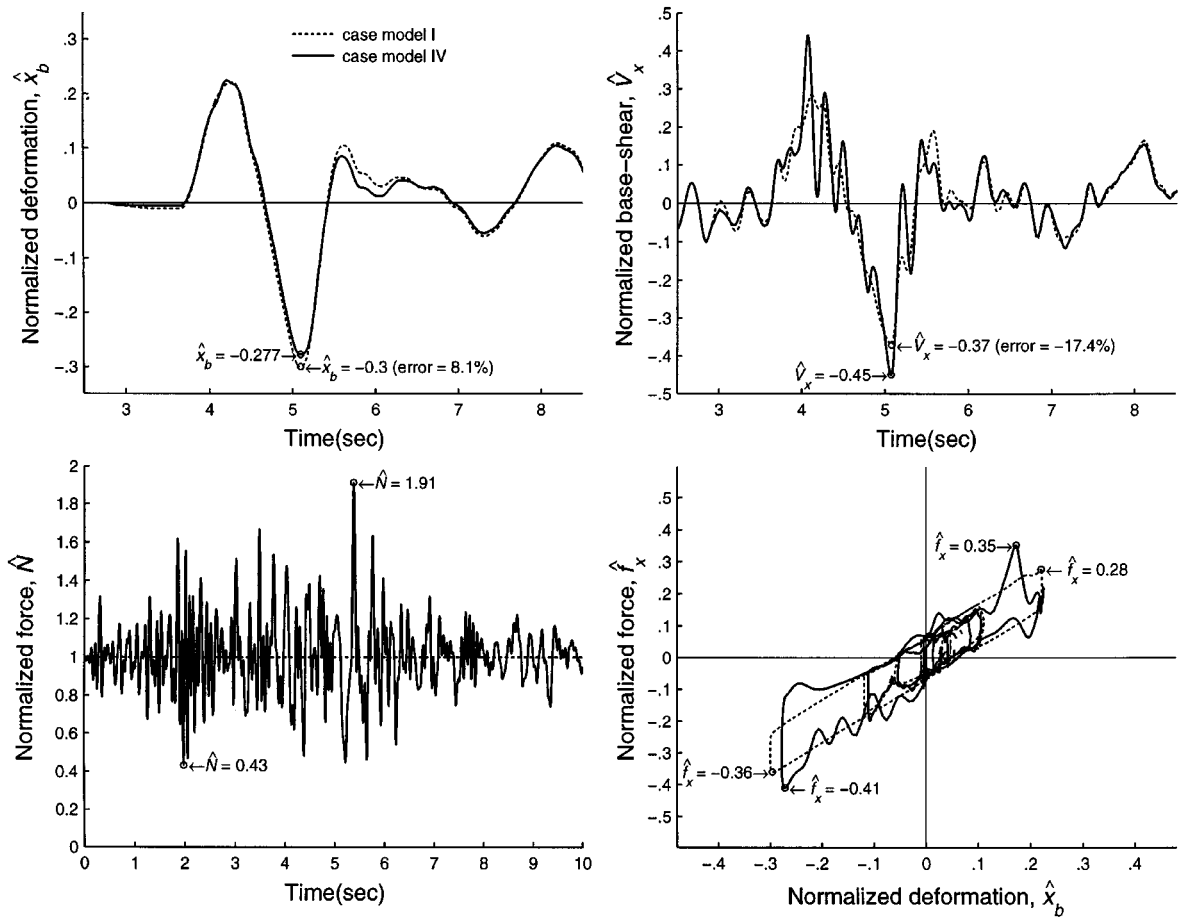

Figure 7. Comparison between earthquake response of case models I and IV subjected to the Newhall ground motion ($T_o = 0{\cdot}5$ sec, $\beta = 7$, $\alpha = 0{\cdot}2$)

with peak errors of about 8 per cent. However, the inclusion of the vertical ground motion component and the complete dynamics of the system in the 'exact' model, leads to structural peak shear values significantly larger (17·4 per cent) than obtained from the simplified model. Such is also the case with the normal contact force $\hat{N}$, which reaches a maximum 91 per cent larger than the corresponding unitary value predicted by the simplified model. The effect of the vertical ground motion component is also apparent in the waviness of the force–deformation loop presented. As it was mentioned earlier, the spikes of these loops result from an increase in the normal contact force due mainly to the vertical ground motion component; peak errors in the FPS force range between 13 and 20 per cent.

An interesting aspect of Figure 7 is that the peak value of N, and hence of $\mathbf{f}$ (equation (2)), tend to occur at large values of the lateral deformation of the FPS. This implies an increase in the maximum value attained by the horizontal FPS restoring force $\mathbf{f}$, which in turn leads to an increase in the maximum base shear of the structure. This increase is due to the simultaneous occurrence of the maximum lateral deformation and a peak positive vertical acceleration of the structure. It so happens that this simultaneous occurrence is indirectly related to the statistical correlation between horizontal and vertical ground motion components. Results from this study show that ground motion components with horizontal to vertical correlation larger than about 0·15 will tend to present this effect.[8]

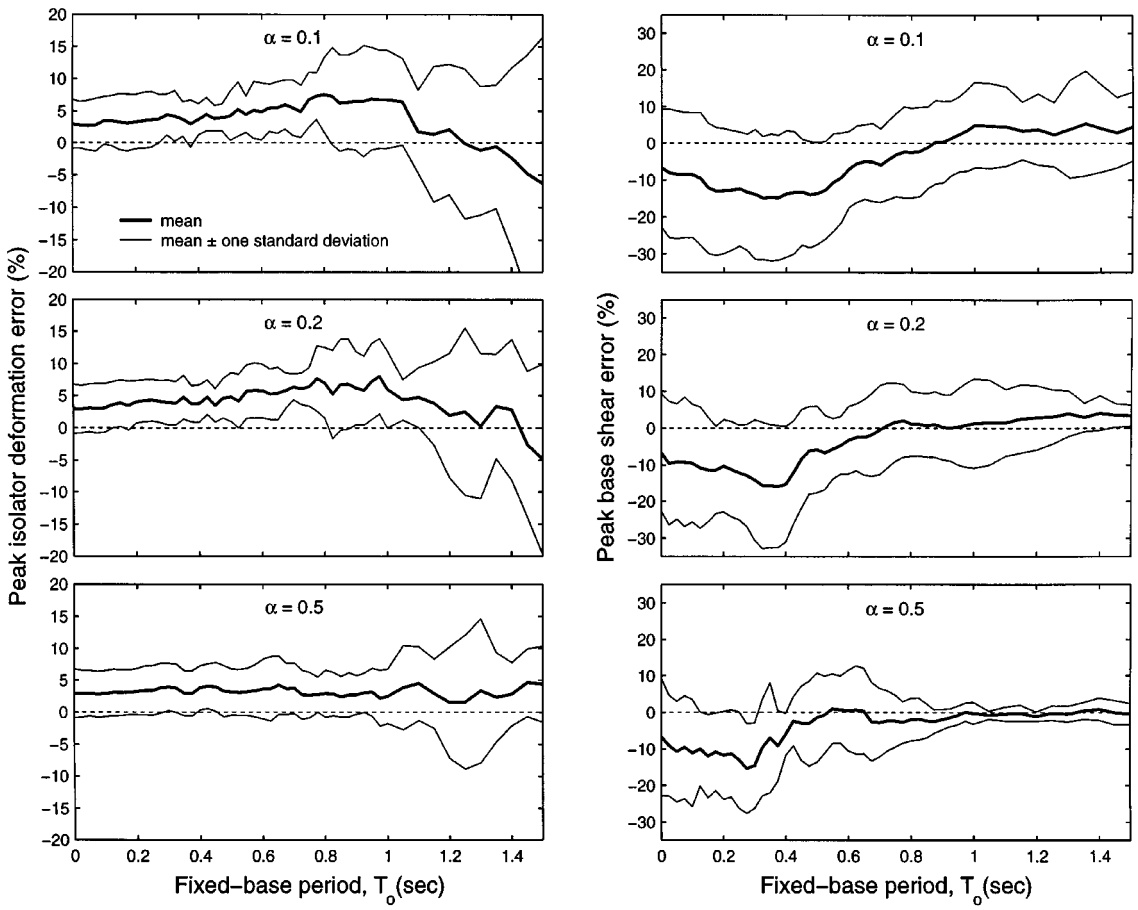

Figure 8. Peak deformation and base shear error spectra for the six ground motions considered using case model I ($\beta = 7$)

Mean and mean plus (minus) one standard deviation spectra of the errors in isolator deformations and structure base shear—of case model I relative to IV—for the six ground motions considered are presented in Figure 8. Mean deformation errors are usually less than 5 per cent and, hence, are reasonably predicted by the approximate model. Mean plus one standard deviation deformations are usually less than 15 per cent; the variation increases with increasing period. The errors are usually positive indicating that the simplified model predicts larger values than the 'exact' model. On the other hand, mean values of base shear are underestimated by less than 10 per cent using the approximate model. Mean-plus-one standard deviation results show underestimations of base shear as large as 30 per cent. Indeed, these variations may be as large as 40 per cent for specific ground motions where correlation exists between the lateral and vertical ground motion components.

The accuracy of intermediate structural case models II and III presented earlier in Table I is evaluated relative to the exact case model IV. Shown in Figure 9 are the error spectra corresponding to each of the four models used to compute the isolator deformation and base shear in the structure subjected to three of the six ground motions considered. As shown in the figure, the accuracy of the different building models is dependent on the ground motion selected. For instance, errors in isolator deformations range in general from 0 to 20 per cent, and are less than 15 per cent for structures with fixed-base period less than 1 sec. These

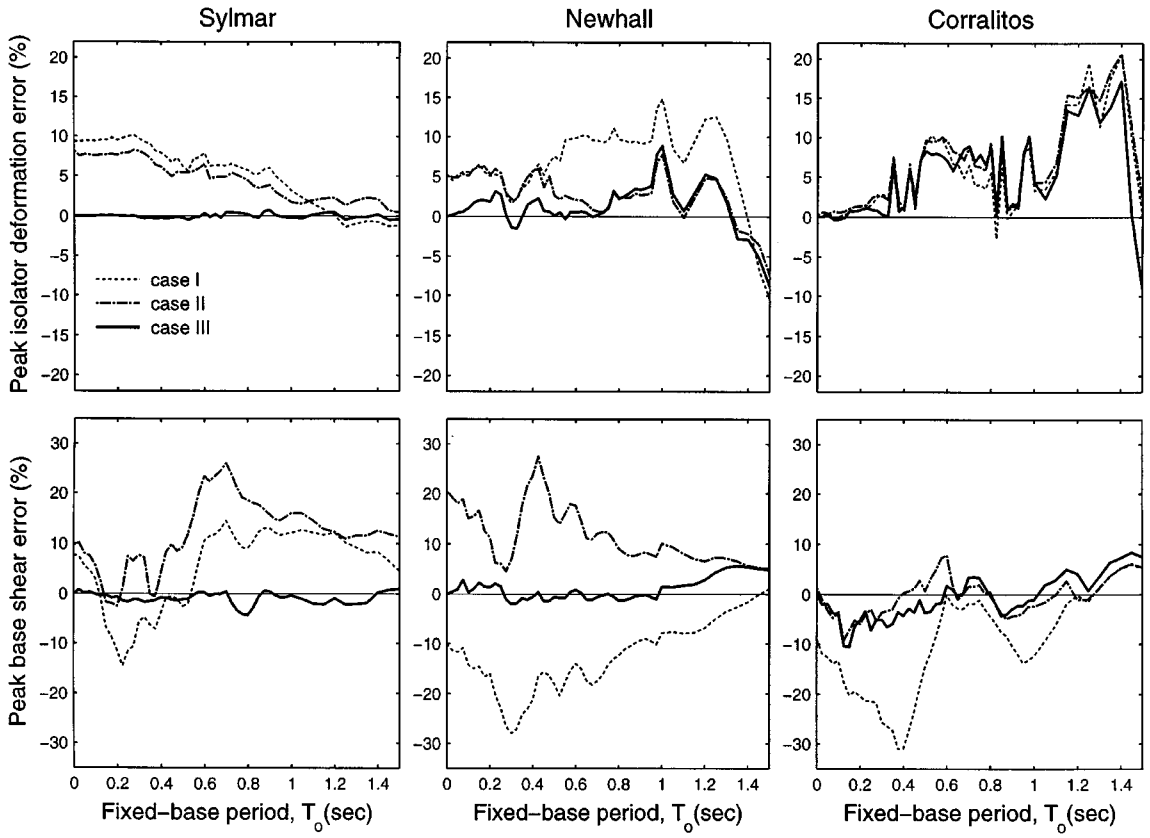

Figure 9. Peak deformation and base shear error spectra for the structural models considered in Table I subjected to Sylmar, Newhall and Corralitos ($\beta = 7$, $\alpha = 0{\cdot}2$)

prediction errors in deformation occur almost always in the safe side, i.e., simplified models tend to overestimate the isolator deformation demand. On the other hand, the predicted base shear by simple models can be either smaller or larger than the actual base shear depending on the model and ground motion considered. For instance, case model II tends to overestimate the base shear in presence of large deformations as produced by the Sylmar and Newhall ground motions. Prediction errors are as large as 30 per cent and tend to be larger for structures with fixed-base period less than 1 sec. Results are in general insensitive to the vertical-to-lateral stiffness ratio β,[8] for typical building values of this parameter (say greater than 5). This does not imply, however, that the vertical dynamics of the FPS could be neglected; it rather implies that the most relevant effects in the vertical motion of the system results from the consideration of the vertical ground motion component and the lateral–vertical coupling induced by the sliding on the spherical surface.

Another final aspect considered is the effect of bidirectional input motion. Shown in Figure 10 is a comparison between the predicted earthquake response of a structure with parameters $T_o = 0{\cdot}3$ sec, vertical to lateral stiffness ratio $\beta = 7$, mass ratio $\alpha = 0{\cdot}2$, and subjected to the Corralitos ground motion. Results are presented for the 'exact' structural model. The peak deformation of the isolation level when the analysis of the structure is performed in the y-direction will be denoted as y_{bo}. Given the symmetry of the FPS system, this radial deformation is presented as a circular boundary (Figure 10) in the deformation space described by the horizontal deformation of the base. Superimposed to that boundary is the response of the structural model subjected to both horizontal ground motion components. Thus, FPS deformations beyond the circular boundary of radius y_{bo} represents an increase in the actual deformation due to the bidirectional

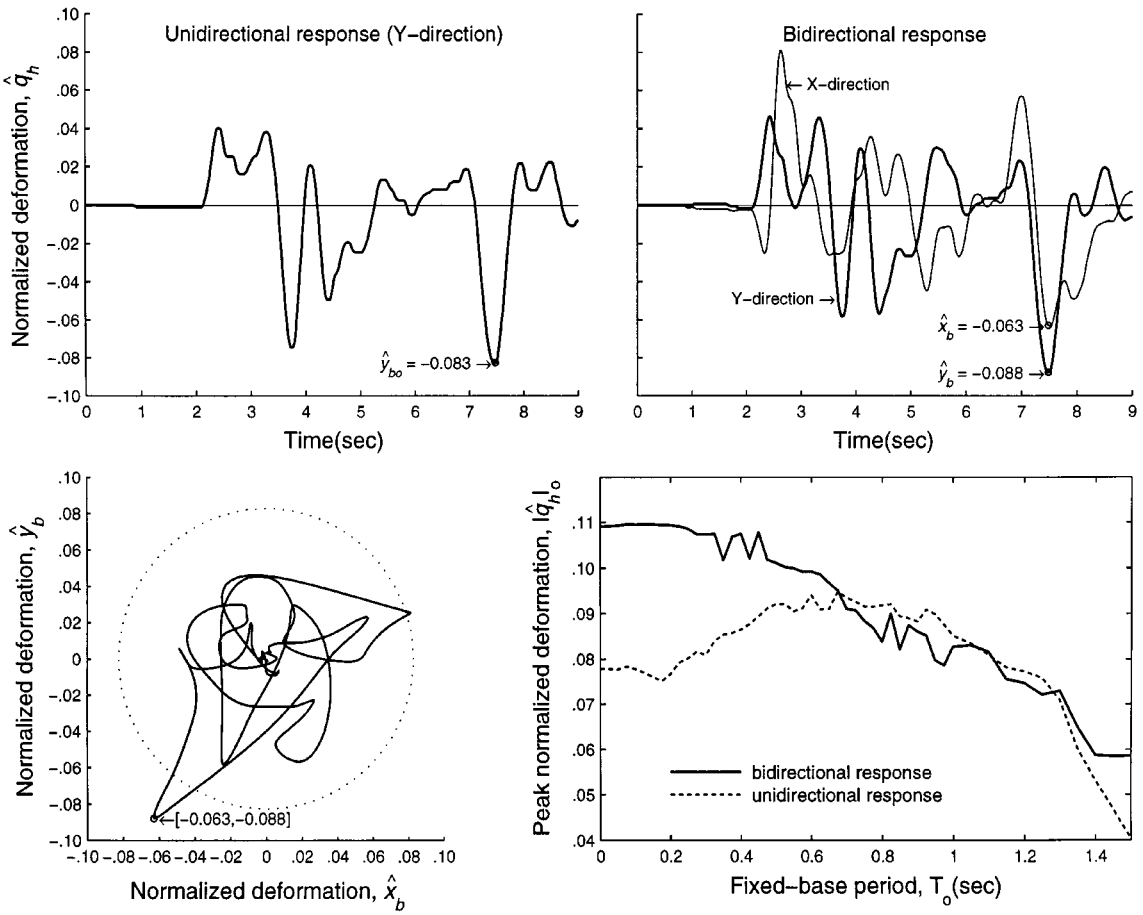

Figure 10. Comparison between the unidirectional and bidirectional earthquake response of the system ($T_o = 0{\cdot}3$ sec, $\beta = 7$, $\alpha = 0{\cdot}2$) subjected to the Corralitos ground motion

input motion. Also presented in the figure is a comparison between the FPS deformation spectra for a single (dashed-line) and bidirectional (solid line) ground motion components. The errors obtained by ignoring the effect of bidirectional ground motion may be as large as 30 per cent in this case, and are specially large for stiff structures, which are precisely those most adequate for the use of an isolation system.

In order to generalize these results, error spectra were computed using the 'exact' model for the six ground motion records considered in this investigation. The mean and mean plus (minus) one standard deviation error spectra are presented in Figure 11 for three different values of the mass ratio, $\alpha = 0.1$, 0.2, and 0·5, and vertical to lateral stiffness ratio $\beta = 7$. It is apparent from the figure that errors of ignoring the two ground motion components in the analysis are larger for rigid structures and decrease steadily with increasing period. Mean errors in the estimated FPS deformations are about 20 per cent; mean plus (minus) one standard deviation may be as large as about 38 per cent. These results seem to be rather insensitive to the vertical-to-lateral stiffness ratio β.[8]

A PHYSICAL MODEL OF THE FPS

So far, the FPS isolator has been assumed to stay at all times in contact with the concave sliding surface during the earthquake. To include the possible uplift and impact between the structure and sliding surface, it

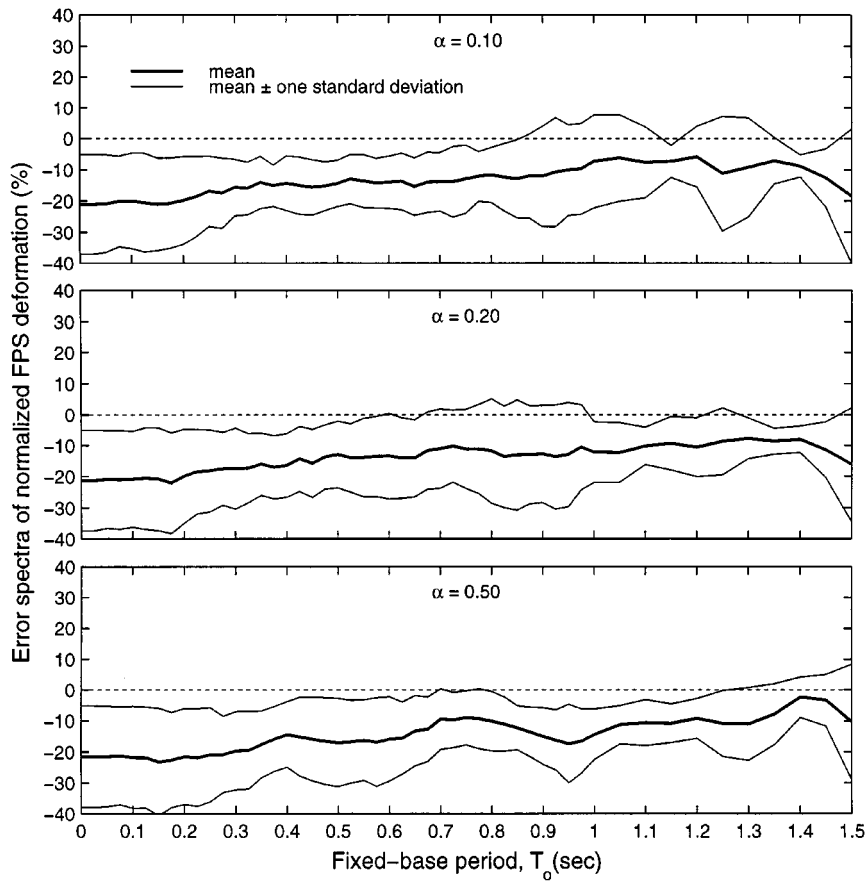

Figure 11. Error spectra of normalized FPS horizontal deformation (vectorial) for the six ground motions considered ($\beta = 7$, $\alpha = 0{\cdot}1$, $0{\cdot}2$ and $0{\cdot}5$)

becomes useful to define a physical model of the FPS isolator that simplifies significantly the analytical formulation and solution of this problem—otherwise such solution would be unnecessarily cumbersome. The only addition of this model relative to the one presented in Figure 2 is that it considers a uniaxial gap element between isolator and the sliding surface. By knowing the force in such element it is possible to keep track of the uplift and impact of individual isolators.

The form in which isolator uplift is modeled deserves special attention. Most commonly, isolator uplift will occur in few isolators rather than all simultaneously. In that case, a formulation based on relative coordinates to the ground is appropriate. Such formulation implies that the position of the sliders relative to the sliding surfaces is known at all times, and so is the position where the slider comes in contact again with the sliding surface after uplift. In the unusual case that all sliders undergo uplift, the formulation of the problem should be based in absolute coordinates in order to known the exact position and velocity of the ground and structure at the time of impact between the two. As conventionally done, a restitution coefficient is introduced to account for the energy loss during the impact in the corresponding isolators.

For the sake of brevity, the analytical formulation of the physical model will be omitted here since it will be presented in a follow-up paper. However, it seems appropriate to comment on the advantages and limitations of such model. The most obvious advantage of the physical model is that enable us to compute the normal contact force N in a simple way. The force developed in the vertical gap element corresponds to

the vertical component of the total reaction **R** acting on the slider (Figure 1(c)). Since we know the direction of **R** and one of its components (the vertical one), this reaction can be simply determined. Moreover, this model is capable of simulating the uplift and impact of the slider through the gap element. It only requires that the integration step be adapted dynamically at the instances of impact to attain sufficient accuracy. The main disadvantage of the model is the existence of a high vertical frequency associated with the large vertical stiffness of the isolator, which requires of an unconditionally stable integration procedure to avoid stability problems in obtaining the solution. Another interesting advantage of this physical model, is that it allows to consider the FPS as a typical non-linear element, in which the input is the deformation and velocity and the output is the restoring force **f**. Thus, this physical model can be incorporated into a conventional structural inelastic analysis program by considering both, the lateral degrees of freedom of the superstructure and base, and the vertical degrees of freedom of each isolator.

In order to understand the 'actual' performance of structures isolated with the FPS, i.e., including effects such as large deformations, uplift, impact, and the true vertical dynamics of the system, the building example presented in Figure 2(b) was studied in detail. The structure is a typical four-storey and two bay reinforced concrete frame with fixed-based fundamental period $T_o = 0{\cdot}53$ sec, constant modal damping ratio $\xi = 0{\cdot}05$, and $\mu = 0{\cdot}07$. Two structural cases are considered: (1) a system that includes the foundation beams presented in Figure 2(b) (30 cm × 70 cm) and having mass ratio $\alpha = 0{\cdot}25$, and (2) a system without the foundation beams and having $\alpha = 0.^7$ The structure is supported on three FPS isolators with radii $R = 100$ cm, leading to a nominal isolated period of 2 sec in both structural models; the resulting β values for the two structures considered are 10 and 13, respectively. As conventionally assumed, beams in the structure were considered axially rigid, implying a single horizontal degree of freedom per building floor. Foundation beams, however, were considered with their nominal axial as well as bending stiffness in order to avoid unnecessary simplifications at the isolation interface. Furthermore, all vertical as well as rotational degrees of freedom were considered in the structure and a consistent mass formulation was used in order to keep the dynamic model as close to reality as possible. A seismic weight of 10 kN/m^2 was considered in every storey of the model; also, a coefficient of restitution $c_r = 0{\cdot}9$ was considered in modeling the isolator impact. As before, two structural models were analysed, one denoted as 'exact' which includes all the above modelling assumptions and one denoted as 'approximate' which ignores the vertical dynamics as well as the overturning of the building. These two cases are equivalent to case models I and IV presented earlier in Table I but extended to the multistorey case.

An important aspect in the modelling of this system is the consideration of gravitational loads. First, a static vertical load analysis of the structure was performed to compute all member forces including the ones in the gap elements of the FPS isolators. The results of that analysis determined a pre-compression condition for the gap elements, necessary in order to check the uplift of individual isolators. Of course, the acceleration of gravity g needs to be included in the vertical dynamics of the problem; indeed, this acceleration is responsible for bringing back to the ground the isolator and structure after been uplifted.

The dynamic response of the system subjected to the Newhall record is presented in Figures 12 and 13 for both values of mass ratio $\alpha = 0{\cdot}25$ and 0. Although results are presented here only for the Newhall ground motion record, the trends observed in this case carry on to other near-field input motions with a strong initial acceleration pulse, such as Sylmar; they are also observed but in a lesser degree for higher-frequency motions such as Llolleo and Viña. There are a number of interesting and practical issues in these figures that should be accounted for in the design of structures supported by FPS isolators.

First, it is observed that discrepancies between the x-direction isolator deformations of the two structural models are small, less than 6 per cent, which is consistent with the results presented earlier in Figure 9. Such discrepancy increases to about 32 per cent when considering the base shear in the structure, which is also consistent with the trends observed for the single FPS system (Figures 8 and 9). Second, it is interesting to observe that uplift occurs in isolators under columns 1 and 3, as it is shown by the zero normal force attained in these isolators at different instants of time. Uplift is identified at several instants of the response in spite of the rather large seismic mass considered and the small height-to-base aspect ratio of the structure. Notice

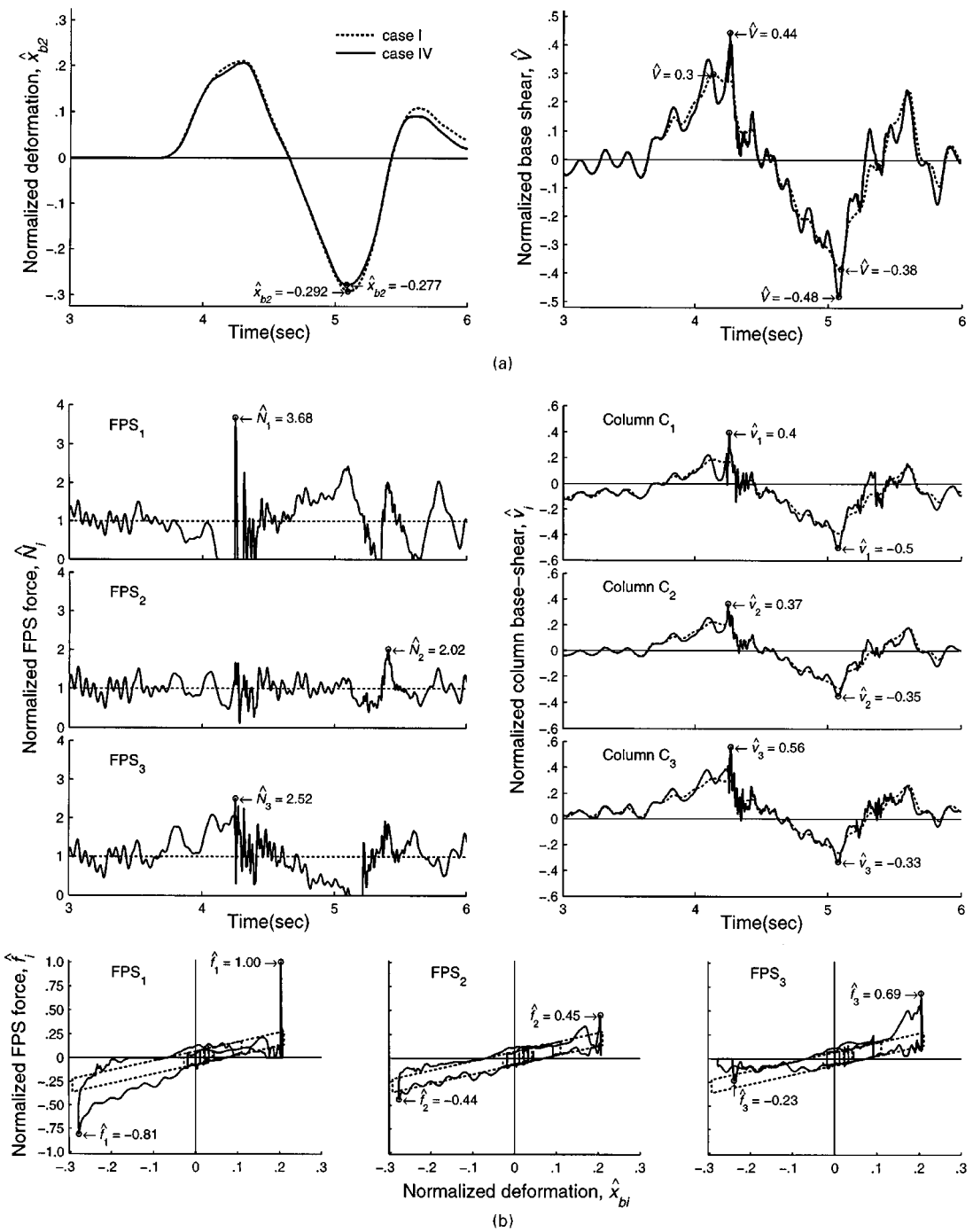

Figure 12. Earthquake response of four-storey frame subjected to the Newhall ground motion ($T_o = 0{\cdot}55$ sec, $\beta = 10$, $\alpha = 0{\cdot}25$, and $c_r = 0{\cdot}9$). (a) global response; (b) column and FPS forces

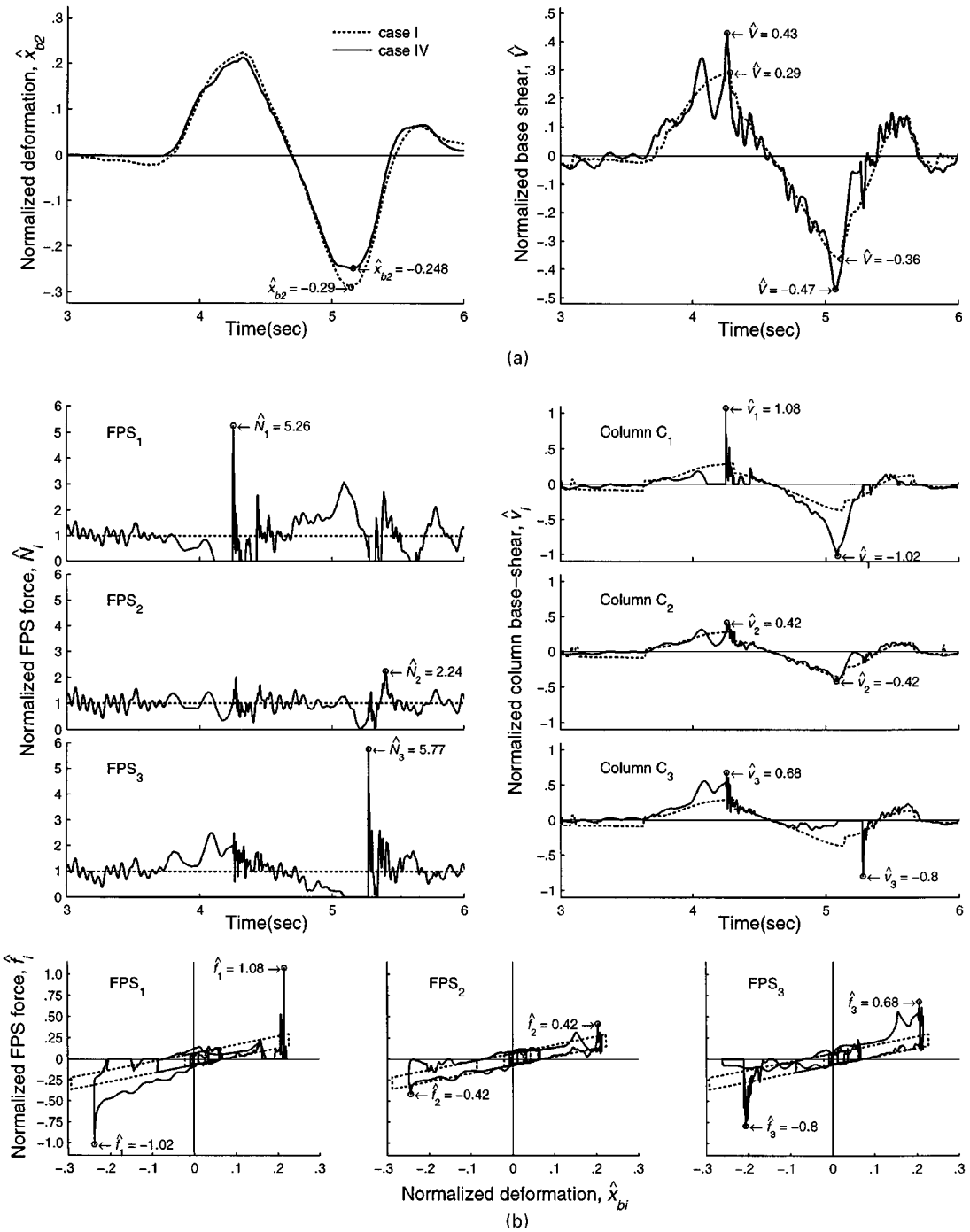

Figure 13. Earthquake response of four-storey frame subjected to the Newhall ground motion ($T_o = 0{\cdot}71$ sec, $\beta = 13$, $\alpha = 0$, and $c_r = 0{\cdot}9$). (a) global response; (b) column and FPS-forces

that uplift and impact occur simultaneously with the largest isolator deformation (see the bottom force deformation loops). As a result of the uplift and downward impact, the maximum normal contact force N ranges from 2 to 3·7 times the actual gravitational load in the isolators of the structure with $\alpha = 0{\cdot}25$ and from 2·2 to 5·8 times the dead load in the isolators of the structure with $\alpha = 0$. More important, the shear in the building columns is increased significantly due to the increase in the normal contact force N and, hence, in the FPS horizontal restoring force **f**. Columns shears range from 0·37 to 0·56 times the dead load in the columns in the first system, leading to an increase of over 50 per cent relative to the estimated shears using the simplified model. Such effect is dramatically increased in the structure with $\alpha = 0$ as a result of not having the filtering action caused by the base mass and the lateral restraint of the foundation beams responsible for the uniform distribution of the base shear among columns. The values of column shear in the latter case range from 0·42 to 1·08 times the dead load in the columns, which represents a peak increase of about 300 per cent over the column shear values obtained from the simplified model. Such large column base shears result from the instantaneous sticking produced in the isolator due to the increase in the normal contact force resulting from the downward impact and overturning of the structure.

Third, it is interesting to note by comparing Figures 12 and 13 that although global building responses, such as base deformations and building base shear are similar in both structures analyzed, element responses, such as individual isolator deformations are substantially different between the two structures considered. The already mentioned effect of instantaneous isolator sticking, due to the increase in normal force as a result of impact and overturning, implies a fixed-base condition for the corresponding column at that instant. If this occurs while the structure without the foundation beams is displacing in one direction, the drift in the column that sticks may be increased considerably. Indeed, such column drift is almost 3 times larger in the latter.

CONCLUSIONS

This investigation about modelling aspects of the FPS system has led to the following conclusions:

The predicted global response quantities, such as isolator and building deformations, obtained from the different structural models considered in this investigation, are in general very similar. For instance, the simpler methods overestimate these deformations in the mean by about 5 per cent. This conclusion agrees with the results of previous analytical and experimental investigations.[3, 4, 7]

Larger discrepancies among models are observed, however, in building base shear and drift. In estimating such response quantities, the first key decision that needs to be made by the engineer involves estimating the degree of correlation between the horizontal and vertical ground motion components for the given site of the structure. If such correlation is expected to be small in absolute value, say less than 0·15, a simpler structural model such as model 1 in Table I can still be used within 15 per cent error. However, the errors in the estimated building base shear using model 1 and for structures subjected to correlated ground motion components, may be as large as 30 per cent. Therefore, case models 2–4, which include the effect of the vertical ground motion component, need to be considered in this case.

Moreover, if isolator deformations larger than about 15 cm are expected, models 3 and 4 (Table I) including a vertical ground motion component and large deformations, should be used for dynamic analysis of the structure. Although case model 3 is approximate, it leads to results that lie within 10 per cent error relative to the exact solution obtained from model 4.

In such case also, estimations of member forces and deformations, should always be obtained from models 3 and 4, or alternatively, from a physical model like the one presented herein.

Normal contact forces during an earthquake may vary in the mean from one-fifth to twice the axial load due to gravitational loads. This increase may be as large as 5 if there is uplift in the isolators resulting from overturning of the structure and vertical ground acceleration. The resulting vertical impact of the slider and the spherical surface leads to two effects that need to be evaluated carefully.

First, column base shears may increase due to the increase in normal force at the isolator interface due to overturning and vertical impact. The resulting instantaneous increase in normal force makes the slider to stop from sliding and to transmit significantly larger shear forces to the supported columns. The effect becomes more important when the mass of the isolation system is small and there are no foundation beams (or a slab) connecting the isolators. It then seems advisable that independently isolated columns be braced and interconnected by a significant mass at the isolation interface capable of filtering the large increase in normal force due to the potential vertical impact resulting from uplift.

Second, variations in the normal contact force lead also to non-uniform drift demand among unbraced building columns due to the sudden restriction to sliding encountered by the columns with increased N. Consequently, uplift should be impaired in order to avoid such localized increase in drift demand.

The Frictional Pendulum System is a reliable device to reduce the earthquake demand on a structure. However, although local effects such as the variation in normal contact forces, large deformations, and uplift do not seem to affect considerably the global system response, they must be considered in the isolation modelling and design, especially for near-field earthquakes with a strong initial acceleration pulse and for statistically correlated horizontal and vertical ground motion components.

ACKNOWLEDGMENTS

This investigation has been funded by the Chilean National Research Fund for Science and Technology, FONDECYT through Grant No. 1950987 and No. 1971078, and by the National Fund for the Foment of Science and Technology, FONDEF through Grant No. D96I1008. The authors are grateful for this support.

REFERENCES

1. M. Constantinou, A. Mokha and A. Reinhorn, 'Teflon Bearings in Base Isolation, Part II: Modeling', *J. Struct. Engng. ASCE* **116**, 455–474 (1990).
2. A. Mokha, N. Amin, M. Constantinou and V. Zayas, 'Seismic isolation retrofit of large historic buildings', *J. Struct. Engng ASCE* **122**, 298–308 (1996).
3. V. Zayas, S. Low and S. Mahin, 'The FPS earthquake resisting system', *Report UCB/EERC-87/01*, Earthquake Engineering Research Center, University of California at Berkeley.
4. V. Zayas, S. Low, L. Bozzo and S. Mahin, 'Feasibility and performance studies on improving the earthquakes resistance of new and existing buildings using the frictional pendulum system', *Report UCB/EERC-89/09*, Earthquake Engineering Research Center, University of California at Berkeley.
5. V. Zayas, S. Low and S. Mahin, 'A simple pendulum technique for achieving seismic isolation', *Earthquake Spectra* **6**, 317–334 (1990).
6. A. Mokha, M. Constantinou and A. Reinhorn, 'Experimental study of friction-pendulum isolation system', *J. Struct. Engng. ASCE* **117**, 1201–1217 (1991).
7. T. Al-Hussaini, V. Zayas and M. Constantinou, 'Seismic isolation of multi-storey frame structures using spherical sliding isolation system', *Report NCEER-94-0007*, National Center for Earthquake Engineering Research, State University of New York at Buffalo.
8. J. Almazán and J. De la Llera, 'Lateral and torsional earthquake behavior of structures isolated with the frictional pendulum system', *Report DIE Universidad Catòlica de Chile*, in preparation.

